3512 J. Agric. Food Chem. 2009, 57, 3512–3518
DOI:10.1021/jf900146a

JOURNAL OF AGRICULTURAL AND FOOD CHEMISTRY
ARTICLE

A Double Mutation in the Anthocyanin 5-*O*-Glucosyltransferase Gene Disrupts Enzymatic Activity in *Vitis vinifera* L.

László Jánváry,[†] Thomas Hoffmann,[†] Judith Pfeiffer,[§] Ludger Hausmann,[#] Reinhard Töpfer,[#] Thilo C. Fischer,[§,⊥] and Wilfried Schwab*,[†]

[†]Biomolecular Food Technology, Technische Universität München, Hochfeldweg 1, 85354 Freising, Germany, [§]Ornamental Plants and Horticultural Plant Breeding, Technische Universität München, Am Hochanger 4, 85354 Freising, Germany, [#]JKI Institute for Grapevine Breeding Geilweilerhof, 76833 Siebeldingen, Germany. [⊥]Present address: Biozentrum der LMU München, Großhadernerstr. 2-4, 82152 Planegg-Martinsried, Germany

The inability of most European grapevines (*Vitis vinifera*) to produce 3,5-di-*O*-glucosides of anthocyanidin-3-*O*-glucosides while in other *Vitis* species diglucosides are found has long been used as a diagnostic tool for the classification of wines according to their varietal origin. A functional 5-*O*-glucosyltransferase (5GT) gene and its nonfunctional allele were recently cloned from the heterozygous hybrid cultivar 'Regent'. Protein sequence comparison revealed only five amino acid substitutions and a truncation at the C-terminus in the inactive enzyme. Restoration of the C-terminus in the European allele alone proved to be insufficient for a reversal to a functional allele. An additional V121L transition located in close spatial vicinity of the catalytically active histidine in the active site of the nonfunctional protein was also essential to recover 5GT activity. Thus, two mutations render the 5GT inactive in *V. vinifera* and explain why revertants for this mutant allele have not been observed in breeding programs. The results have a significant effect on the classification and breeding of *Vitis* varieties and the evaluation of derived products.

KEYWORDS: Anthocyanins; 5-*O*-glucosyltransferase; mutation; malvin; *Vitis*

INTRODUCTION

Grapevines (mainly *Vitis vinifera*) are considered to be one of the oldest cultivated crop plant species as their use is known to date back to the Neolithic period (*1*, *2*). The domestication of the Eurasian grape (*V. vinifera* ssp. *vinifera*) from its wild ancestor (*V. vinifera* ssp. *sylvestris*) has long been claimed to have occurred in Transcaucasia. However, SSR analysis (*3*) and analyses of chloroplast DNA polymorphisms suggest the existence of at least two important origins for the cultivated germplasm, one in the Near East and another in the western Mediterranean region, the latter of which gave rise to many of the current Western European cultivars (*4*). During domestication, the biology of grapes underwent several dramatic changes, for example, selection of hermaphroditic forms, showing increased yield due to increased berry number and berry size as well as larger clusters (*5*). The introduction of the North American pests phylloxera (*Daktulosphaira vitifoliae*, an aphid) and powdery mildew (*Erysiphe necator*, a fungus) into Europe in the mid-1800s was devastating to grape growers. As a consequence, interspecific varieties have been bred to combine the quality of traditional European cultivars with the resistance of American species (e.g., *Vitis rupestris*, *Vitis labrusca*, and *Vitis riparia*), but the wine quality of those hybrids was inferior when compared with that from the traditional cultivars. Because numerous winemakers grew hybrid varieties at the beginning of the 20th century, more and more hybrid wines appeared on the market. To maintain high quality standards, blending of hybrid wines and quality wine was prohibited.

Grapes are cultivated for fresh fruit, dried fruit (raisins), and wine production. For all these uses, color is one of the most important characteristics. It is determined primarily by the genotype, but to some extent also by processing (e.g., rosé wine from red grape cultivars). *Vitis* species and cultivars produce a unique set of anthocyanin pigments (*6*). Oenin (malvidin 3-*O*-glucoside) is the major anthocyanin of red European *V. vinifera* cultivars, whereas most other *Vitis* species or their hybrids produce malvin (malvidin 3,5-di-*O*-glucoside), which is consequently used as a simple diagnostic tool to determine if a "nonvinifera" species has been used in red winemaking (**Figure 1**) (*6*−*9*). Only traces of anthocyanidin 3,5-di-*O*-glucosides are found in some red European cultivars (*10*, *11*). Whereas 3-*O*-glucosylation is generally required for anthocyanidin stabilization, the additional 5-*O*-glucosylation occurs only in a few plant taxa.

Recently, cDNAs for putative 5-*O*-glucosyltransferase (5GT) genes were cloned from *Vitis* cultivars and two presumed anthocyanin 5GT nucleotide sequences (*5GT-Dia* and *5GT-Cha*) were isolated from BACs of cv. 'Regent', which is a cross between the European *V. vinifera* cv. 'Diana' and the interspecific hybrid cv.

*Corresponding author [telephone +49(0)8161712912.; fax +49(0)8161712950; e-mail schwab@wzw.tum.de].

 Published on Web 4/1/2009

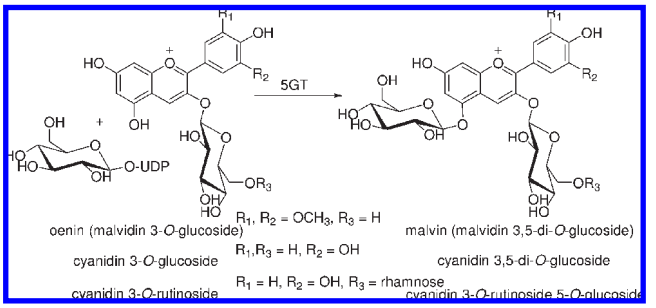

Figure 1. Reactions catalyzed by 5-glucosyltransferase (5GT).

'Chambourcin', showing a complex descent of eight *Vitis* species including *V. vinifera* (http://ec.europa.eu/agriculture/markets/wine/studies/vine_en.pdf, Hausmann et al., unpublished data). Functional analysis of the recombinant proteins encoded by the two orthologous *5GT* genes showed that 5GT-Cha glucosylates efficiently malvidin 3-*O*-glucoside at the 5-position, whereas 5GT-Dia is inactive. Loss-of-function of *5GT-Dia* in European *V. vinifera* with its significant consequence for wine anthocyanins was studied by site-directed mutagenesis and functional tests with the recombinant enzymes.

MATERIALS AND METHODS

Materials. UDP-glucose was obtained from Sigma-Aldrich; malvidin 3-*O*-glucoside and cyanidin 3-*O*-glucoside were obtained from Extrasynthese (Genay, France); cyanidin 3-*O*-rutinoside, cyanidin 3,5-di-*O*-glucoside, and malvidin 3,5-di-*O*-glucoside were obtained from Roth (Karlsruhe, Germany). Solvents and other chemicals were of analytical grade and were obtained from Sigma-Aldrich, Fluka, Riedel de Haën (all Taufkirchen, Germany), Merck (Darmstadt, Germany), or Roth (Karlsruhe, Germany). Precoated cellulose TLC plates were from Merck. Enzymes and reagents for DNA manipulation were from Fermentas (St. Leon-Rot, Germany).

Site-Directed Mutagenesis. PCR/ligation-based site-directed mutagenesis was performed using a straightforward method. In brief, two adjacent (but not overlapping) fragments upstream and downstream of the mutagenesis site were amplified with *Pfu* DNA polymerase in two separate reactions with each an external primer (beyond the N- and C-termini of the gene) and each a ligation point primer (with the site of later ligation close to or directly at the mutagenesis site). Only one of the primers at the adjacent site was 5′-phosphorylated (to minimize the number of possible ligation products later on). One primer contained the desired nucleotide exchange for mutagenesis (Supporting Information Table S1). PCRs were performed with minimum template concentration (to avoid later function as template after ligation and dilution). One microliter of each PCR reaction was ligated in 20 μL of buffer with 5 units of T4 DNA ligase for 10 min at 25 °C. One microliter of the ligation product was diluted 1:2000 (to save removal of the first template, primer, and remains of the two PCR fragments) and used as template for PCR amplification of the ligated and mutagenized full-length product with *Pfu* DNA polymerase using only the external primers. The ligation point primers for the reverse mutagenesis of the premature stop at codon 425 in *5GT-Dia* to the *5GT-Cha* sequence were *425Crev 5′-P-CAC CTC TTT AAC TCA TCA CTC GTT-3′ and *425Cfor 5′-CTT GGA ATT GGT TAT GGG AGA C-3′, resulting in *5GT-Dia-*425C* (mutated site underlined). To conduct the additional V121L exchange in *5GT-Dia-*425C* the ligation point primers V121Lfor 5′-P-GAT CTA CTC TAT CCT AAT TCC TGG-3′ and V121Lrev 5′-AAA CAA CTG ATG GGG CGA CCT T-3′ were used for site-directed mutagenesis, resulting in the double mutant *5GT-Dia-*425C, V121L*. External primers were 5GTfor and 5GTrev for both constructs, which were also used for preparation of the expression constructs for the native alleles *5GT-Cha* and *5GT-Dia*. Stop codon was introduced into *5GT-Cha* at the position corresponding to the premature stop codon in the *5GT-Dia* allele using C425* 5′-CCA ATC ACC TCT TTA ACT CAT CAC TC-3′ as reverse primer for amplification in combination with the upstream primer 5GTfor.

Preparation of Expression Constructs. Expression constructs were prepared in the pYES2.1/V5-His-TOPO vector (Invitrogen, Karlsruhe, Germany) but without employing the His-Tag function. The two native 5GT sequences were derived from the VvB12H3 and VvB21G4 BAC clones that carry the 'Chambourcin' allele 5GT-Cha and the 'Diana' allele 5GT-Dia, respectively (Hausmann et al., unpublished data). The mutagenized and ligated PCR fragments were amplified with the same external primers 5GTfor 5′-CAC TTT CCA CCT GAG ACA CC-3′ and 5GTrev 5′-CAG TAC ATC AAA CGC CAC TC-3′ designed from the upstream and downstream noncoding regions of the Chambourcin allele, as for the two native 5GT sequences. One unit of Taq DNA polymerase for 10 min at 72 °C provided the 3′ overhanging "A" for T/A cloning after PCR had been performed with the proofreading *Pfu* DNA polymerase. The amplified PCR products were cloned into the pYES2.1/V5-His-TOPO vector (Invitrogen). Constructs were verified for insert orientation by colony PCR and sequenced by a commercial service (Microsynth AG, Balgach, Switzerland). Competent *Saccharomyces cerevisiae* INV*Sc*1 cells (Invitrogen) were prepared and transformed with the appropriate constructs using the *S. cerevisiae* EasyComp Transformation Kit (Invitrogen).

Expression of Recombinant Enzymes. Recombinant enzymes were prepared from galactose-induced yeast cultures (*12*, *13*). INV*Sc*1 yeast cells containing an empty pYES2 vector (Invitrogen) were used to prepare the negative control.

Assay of Enzyme Activity. Anthocyanidin 3-*O*-glucoside 5-*O*-glucosyltransferase assays were performed in 50 μL of a 100 mM Tris-HCl, pH 7.5, buffer, containing 0.4% sodium ascorbate, 700 μM UDP-glucose, and 10 μL of recombinant enzyme preparation. The reaction was initiated by the addition of 750 μM malvidin 3-*O*-glucoside (820 μM cyanidin 3-*O*-glucoside or 630 μM cyanidin 3-*O*-rutinoside) in H_2O and was stopped and stabilized by the addition of 25 μL of MeOH containing 1% HCl after 1 h at 30 °C.

Analysis of Reaction Products. Twenty-five microliters of the reaction mixture was loaded on precoated cellulose TLC plates and developed in GT mobile phase (water/acetic acid/HCl 82:15:3). Chromatograms were recorded on an Epson Perfection 3590 photoscanner. The identities of the products were confirmed by LC-MS.

LC-MS. A Bruker Daltonics esquire 3000^{plus} ion trap mass spectrometer (Bruker Daltonics, Bremen, Germany) connected with an Agilent 1100 HPLC system (Agilent Technologies, Waldbronn, Germany) equipped with a quaternary pump and a variable-wavelength detector was utilized. Components were separated with a Phenomenex (Aschaffenburg, Germany) Luna C-18 column (150 mm long × 2.0 mm inner diameter, particle size = 5 μm), which was held at 25 °C. Enzyme assays were analyzed using a linear gradient from 100% A (0.1% formic acid in water) to 100% B (acetonitrile) in 30 min with a flow rate of 0.2 mL/min. The detection wavelength was either 360, 520, or 280 nm. The electrospray ionization voltage of the capillary was set to −4000 V and the end plate to −500 V. Nitrogen was used as dry gas at a temperature of 300 °C and a flow rate of 10 L/min. The full-scan mass spectra were measured in a scan range from m/z 50 to 800 with a scan resolution of 13000 m/z/s until the ICC target reached 20000 or 200 ms, whichever was achieved first. Tandem mass spectrometry was carried out using helium as collision gas (3.56×10^{-6} mbar) with the collision voltage set at 1 V. Spectra were acquired in the positive and negative ionization modes. Data analysis was performed using DataAnalysis 3.1 software (Bruker Daltonics).

Protein Modeling. DeepView (http://www.expasy.org/spdbv/) software was used for visualization of the amino acids in the protein models (*14*). Protein homology modeling was performed with CPHmodels 2.0 Server (*22*) (http://www.cbs.dtu.dk/services/CPHmodels/). Amino acid positions are addressed throughout the text according to the numbering of the protein sequence alignment of *V. vinifera* anthocyanidin 3-*O*-glucosyltransferase (VvGT1) and the anthocyanidin 3-*O*-glucoside 5-*O*-glucosyltransferase sequences 5GT-Cha and 5GT-Dia as shown in **Figure 2**.

RESULTS

Search for Potentially Deleterious Mutations. Sequence comparison of the two 5GT alleles of cv. 'Regent' inherited from

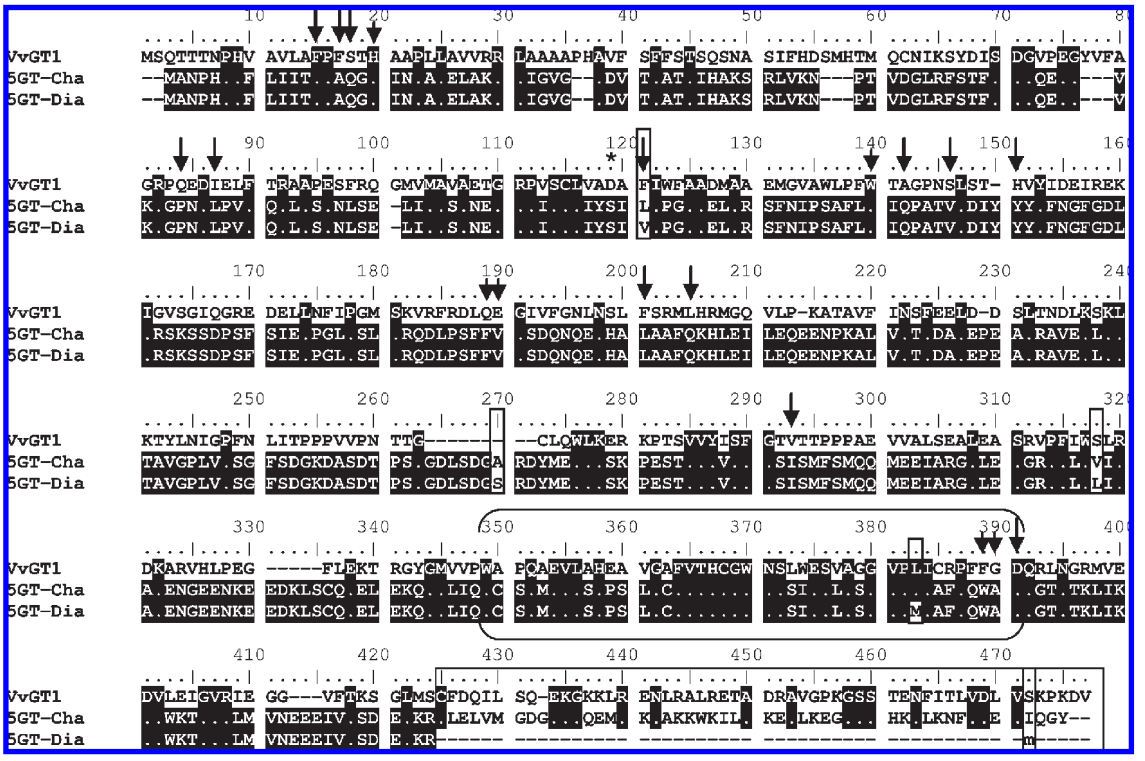

Figure 2. Protein sequence alignment of *Vitis vinifera* anthocyanidin 3-*O*-glucosyltransferase (*VvGT1*) and the functional 5-*O*-glucosyltransferase (*5GT-Cha*) and nonfunctional 5GT (*5GT-Dia*) from *V. vinifera* cv. Regent. The alignment was performed using ClustalX (*31*). Conserved amino acids are shaded, amino acids within 5 Å to quercetin in the protein model of VvGT1 are marked with an arrow, catalytically active amino acids are labeled with an asterisk, and amino acid exchanges in 5GT-Cha and 5GT-Dia are boxed. The positions of the amino acid exchanges in the original sequences are L110V, A259S, V307L, L372M, and I461m. The plant secondary product glucosyltransferase box, characteristic for GTs involved in natural product conjugation, is shown in parentheses.

'Chambourcin' (functional *5GT-Cha*) and 'Diana' (nonfunctional *5GT-Dia*) revealed a number of nucleotide substitutions leading to only five amino acid exchanges in the protein sequence and a premature stop codon at the C-terminus of the 'Diana' allele, which truncates the protein (**Figure 2**). The positions of the five mutated amino acids were compared with the corresponding positions in the sequences of functionally characterized 3′GT from *Medicago truncatula* (UGT71G1 AAW56092) (*15*), 3GT from *Vitis vinifera* (AAB81683) (*16*, *17*), and 5GTs from *Petunia hybrida* (AB027455) (*18*), *Verbena hybrida* (AB013598) (*19*), *Perilla frutescens* (AB013596) (*19*), *Torenia hybrida* (AB076698), *Gentiana triflora* (AB363839) (*20*), *Iris hollandica* (AB113664) (*21*), and the 5GT gene identified in *Arabidopsis thaliana* (UGT75C1 NM_117485) (*22*). The amino acid substitution I472m is irrelevant due to the premature stop after R424 in 5GT-Dia. One amino acid exchange (L383M) occurs in the plant secondary product glucosyltransferase box (PSPG), a region of the protein sequence that is characteristic for natural product conjugation and recognizes the donor molecule UDP-glucose (*15*, *16*). However, L383 is not highly conserved in other functional glucosyltransferases and can be replaced by Ile, Val, or Met as in 5GT-Dia (*15*). Two amino acid substitutions (A270S and V318L) are located in highly variable regions of the amino acid sequence and do not appear to be involved in either donor or acceptor binding (*15*, *16*).

The L121V exchange aligns with F121 of VvGT1, which is located in the immediate vicinity of the catalytically active D119 (**Figure 2**). It has been postulated that the carboxyl function of D119 forms a proton transfer chain with the imidazole residue of H20 to help deprotonate acceptor molecules (*15*). Although D119 is not conserved in functionally characterized 5GTs, F121 is conserved in flavonoid glucosyltransferases from *Fragaria* × *ananassa* (FaGT1 AY663784, FaGT6 DQ289587, FaGT7 DQ289588), *V. vinifera* (VvGT1 AAB81683), and *M. truncatula* (UGT71G1 AAW56092), whereas L121 is conserved in enzymatically active 5GTs except for the *Petunia* protein, which carries a Phe. Thus, besides the restoration of the C-terminus, the site-specific reversal mutation of V121L seemed to be a suitable strategy to regain catalytic activity for 5GT-Dia.

Protein homology modeling with CPHmodels 2.0 Server (*23*) (http://www.cbs.dtu.dk/services/ CPHmodels/) showed that the overall shape of the crystallized VvGT1 (anthocyanidin and flavonoid 3-*O*-glucosyltransferase) protein and the calculated structures of 5GT-Cha and 5GT-Dia are very similar. They consist of two N- and C-terminal domains that are tightly packed and form a deep cleft with the donor and acceptor molecule bound (**Figure 3A**−**C**). Due to the premature truncation, the 5GT-Dia protein lacks 51 amino acids that form two helix structures connected by a loop at the C-terminus (**Figure 3C**). The transition of the loop to the second helix structure contains a G458−S459−S460 motif, which is conserved in all biochemically characterized 5GTs and a number of flavonoid glucosyltransferases (**Figure 2**). Interestingly, in the three-dimensional structure the C-terminus is situated at the opposite site of the cleft, which harbors the catalytic amino acids. It appears that the two helices help to stabilize the spatial structure of the deep cleft by fixing the N- and C-terminal domains.

A detailed inspection of the putative donor binding site reveals that in VvGT1 quercetin stands in a narrow, deep pocket built by five nonpolar amino acids (F15, F121, F201, L205, and F389; **Figure 3D**). The general base H20 responsible for the deprotonation of the acceptor and the donor UDP-glucose are located in proximity to the 3-OH of the acceptor (*15*, *16*). In the

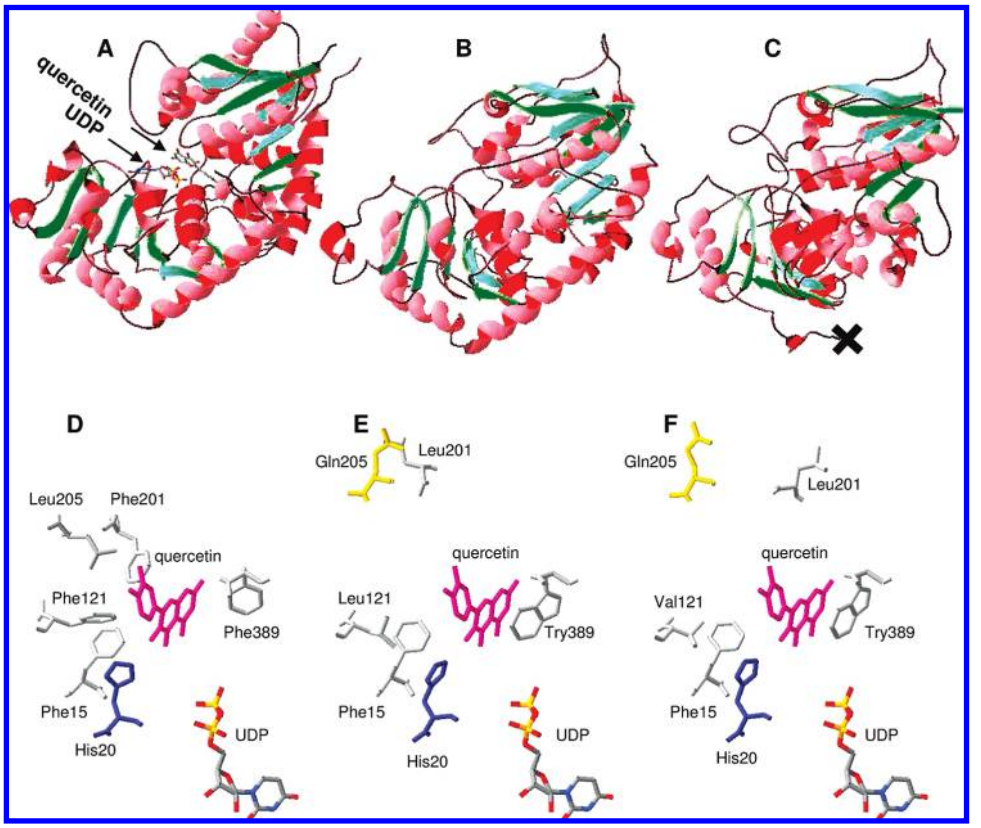

Figure 3. Three-dimensional protein structure of VvGT1 (pdb: 2c9z, **A**, **D**) and calculated protein structures of 5GT-Cha (**B**, **E**) and 5GT-Dia (**C**, **F**) obtained by computer modeling with CPHmodels 2.0 Server [(*22*) http://www.cbs.dtu.dk/services/ CPHmodels/]. Truncation of the amino acid sequence in 5GT-Dia is indicated by a black cross (**C**). UDP (liberated from UDP-glucose) and acceptor (quercetin shown in pink) binding site of VvGT1 (**D**) and calculated active site of 5GT-Cha (**E**) and 5GT-Dia (**F**) are shown. The catalytically active amino acid His20 is shown in blue, nonpolar amino acids are shown in gray, and polar amino acids are in yellow. Figures are drawn with DeepView (*14*).

calculated protein structure of 5GT-Cha, F121 is replaced by L121, whereas 5GT-Dia is mutated in the same position and contains V121 (**Figure 3E**,**F**). Thus, protein modeling studies also confirmed the L121V transition as a potentially deleterious mutation.

Restoration of Enzymatic Activity. To identify deleterious mutations in the *5GT-Dia* allele that render the corresponding enzyme inactive in European *V. vinifera* cultivars, we replaced the premature stop codon in the nucleotide sequence with the codon for Cys (**Figure 4A**). However, although the protein was expressed, the recombinant enzyme (5GT-Dia *425C) remained inactive, being still unable to catalyze the 5-*O*-glucosylation of oenin, cyanidin 3-*O*-glucoside and cyanidin 3-*O*-rutinoside (**Figure 4B**; Supporting Information Figures S1−S3). Consequently, we assumed that an additional mutation might be detrimental in the allelic gene. As a second approach, V121 was mutated to L121 because protein sequence comparison and computer modeling analyses identified this amino acid exchange as the most promising target. The genetically modified protein (5GT-Dia *425C V121L) regained full enzymatic activity (**Figure 4B**; Supporting Information Figures S1−S4). The identities of the products were confirmed by LC-MS (**Figure 4C**; Supporting Information Figure S4). As control, a premature stop codon was incorporated into *5GT-Cha* at position 425 to confirm the deleterious effect of the truncation in 5GT-Dia (**Figure 4A**). The recombinant protein (5GT-Cha C425*), which lacks 51 amino acids of the C-terminus, is inactive (**Figure 4B**; Supporting Information Figures S1−S3). Thus, the other four amino acid exchanges, A270S, V318L, L383M, and I472M, represent silent mutations as they do not affect the 5-*O*-glucosylation. The result clearly demonstrates that the double mutation in the anthocyanin 5-*O*-glucosyltransferase gene (*5GT-Dia*) disrupts enzymatic activity of the encoded protein and explains the inability of such *V. vinifera* cultivars to produce anthocyanidin 3,5-di-*O*-glucosides.

DISCUSSION

We aimed at regaining enzymatic activity in the encoded protein of the *loss-of-function 5GT-Dia* allele by site-directed mutagenesis to identify the essential deleterious mutations in comparison to the active *5GT-Cha* allele of the gene. Abolishment of the premature stop codon with restoration of the C-terminus in the European allele alone proved to be insufficient for a reversal to a functional allele. However, relying on sequence comparison and three-dimensional protein modeling supported by an available crystal structure of a 3GT from *V. vinifera*, a second essential mutation Val121 was identified (Supporting Information Figure S5). Reversal of the base substitution at this site to the codon Leu121 of the American allele, together with the restoration of the C-terminus, resulted in in vitro enzyme activity, obtaining an artificial functional European 5GT allele. Most importantly, this strategy identified two mutations, which gave rise to the biological variation of anthocyanins in American and European grapes. The double mutation in *5GT-Dia* also offers an explanation as to why revertants for this allele have not been reported in breeding programs up to now. Although the crystal structure of three plant glucosyltransferases have been resolved and mutational analysis of the *M. truncatula* glycosyltransferase UGT71G1 and *A. thaliana* glycosyltransferases UGT74F1 and UGT74F2 have revealed residues that control regioselectivity of flavonoid glycosylation, the significance of F121 in the

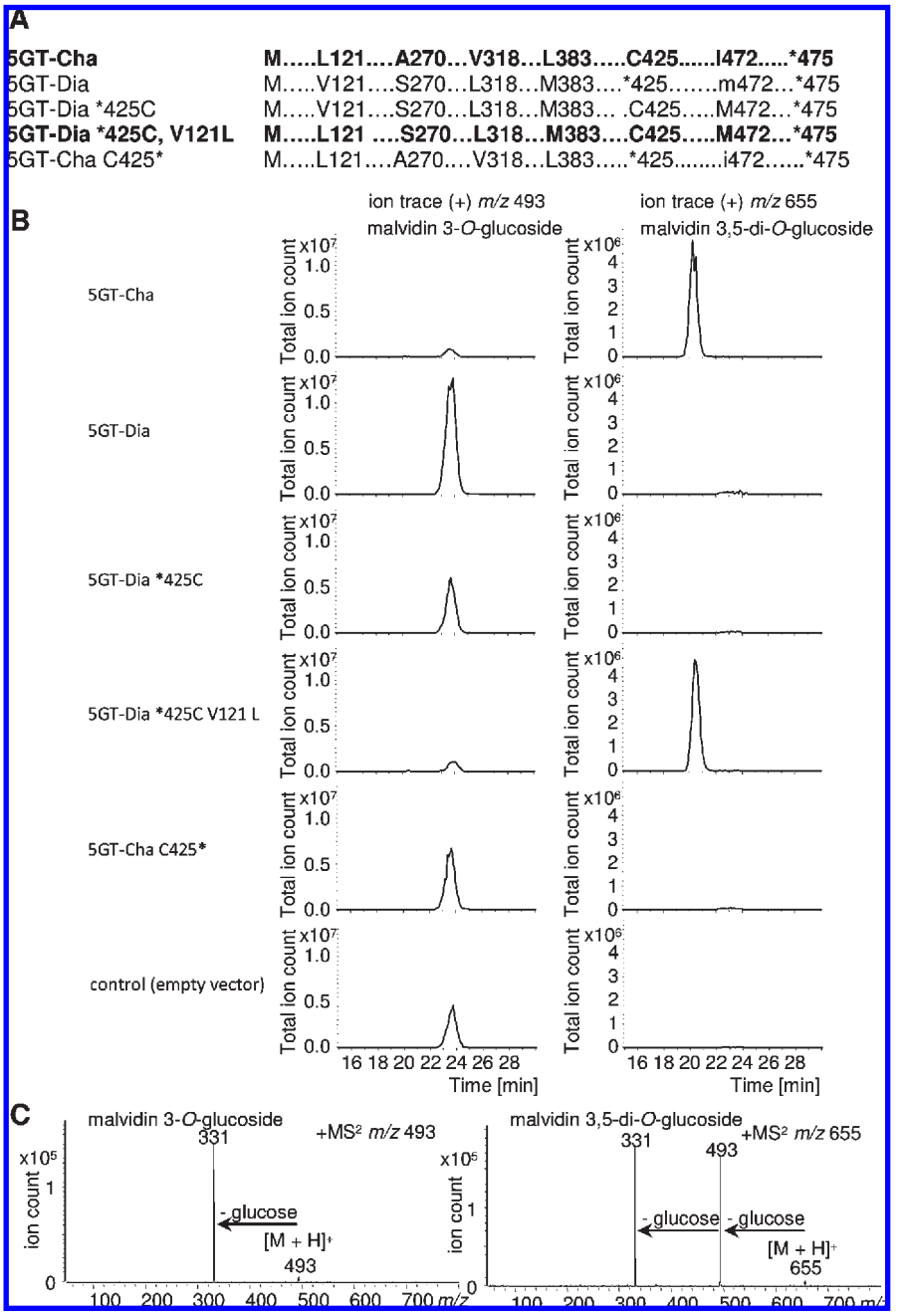

Figure 4. Mutational analysis of 5GTs. Reverse mutagenesis (*425C and V121L) of two deleterious point mutations renders 5GT-Dia active (**A**). Enzymatically active proteins are shown in bold, and asterisks denote stop codons. Small letters indicate amino acids that are not translated due to a premature stop codon upstream of the sequence. The positions of the amino acid exchanges in the original sequences are L110V, A259S, V307L, L372M, and I461m. Product formation (malvidin 3,5-di-*O*-glucoside, pseudomolecular ion *m*/*z* 655) from the substrate malvidin 3-*O*-glucoside (*m*/*z* 493) was demonstrated by LC-MS analysis (**B**). 5GT-Dia, 5GT-Dia *425C, and 5GT-Cha C425* are virtually inactive as no product (malvidin 3,5-di-*O*-glucoside) was detected. The product ion spectra of malvidin 3-*O*-glucoside and malvidin 3,5-di-*O*-glucoside (**C**) are shown.

M. truncatula and *A. thaliana* proteins corresponding to L121 in 5GT-Cha has not been evaluated, being mentioned only as one of the amino acids forming the hydrophobic substrate binding pocket (*15*, *16*, *24*−*26*). It is also remarkable that the exchange of Leu with Val, an amino acid different only in the length of its side chain, at this position can lead to complete loss of enzymatic activity in the 5GT-Dia *425C compared to the 5GT-Dia *425C, V121L, which shows wild type activity.

Most of the wines produced from American species and cultivars have a strong, characteristic musty flavor and aroma, which is disagreeable to many wine consumers. Despite intensive grape breeding, this "foxy" flavor still hampers production of European style wines from native American grapes. Methyl anthranilate has been suggested as an important component of the characteristic *V. labrusca* aroma and has been implicated as a contributor to "foxiness" in American wines (*27*). Recently, it has been shown that the biosynthesis of methyl anthranilate involves an alcohol acyltransferase gene, anthraniloyl-CoA:methanol anthraniloyl transferase (*AMAT* AY705388 (*27*)). Methyl anthranilate and related volatile compounds were also identified in 'Pinot Noir' wines as minor constituents, below the sensory threshold (*28*, *29*). The protein CAO23156, the most similar *V. vinifera* homologue of AMAT, with 95% identity on the amino acid level, is encoded on chromosome 9 of 'Pinot Noir' PN40024, as well as the 5GT (**Figure 5**). Colocalization of the two genes would explain the observed correlation between the ability

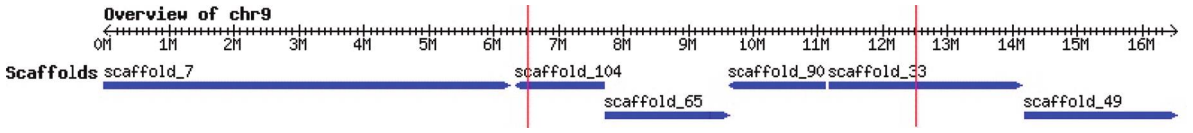

Figure 5. Localization of the 5-glucosyltransferase and an AMAT homologue in one linkage group. Overview of the chromosome 9 of *Vitis vinifera* 'Pinot Noire' PN40024. Red marking in scaffold_104: nucleotide sequence CU459321:1182591..1183985 identical with the 5GT-Dia allele is located on chr9 scaffold_104. GenBank Accession CU459321, version CU459321.1 GI:157356496. Red marking in scaffold_33: *V. vinifera* unnamed protein CAO23156 is located on chr9 in scaffold_33. CAO23156 locus_tag="GSVIVT00025220001"/coded_by="complement (join(CU459250.1:1342510..1343412, CU459250.1:1344103..1344549). CAO23156 is 95% identical on the amino acid level with *V. labrusca* anthraniloyl-CoA:methanol anthraniloyl transferase (AMAT). AMAT GenBank Accession AY705388, protein_id AAW22989. AMAT catalyzes the formation of methyl anthranilate, which is responsible for the "foxy" aroma of the Concord grape (*V. labrusca*). The figure was constructed from images made using the Grape Genome Browser on http://www.genoscope.cns.fr/externe/GenomeBrowser/Vitis.

to form "foxy" flavor and the presence of anthocyanidin 3,5-di-*O*-glucosides in *Vitis* sp. hybrids, based on genetic linkage.

Besides, American species have been used in European grape-breeding programs as a source of disease resistance genes. Most of the wines produced from the descendents have strong and characteristic off-flavors, which are strictly refused by consumers. Monitoring of malvin (malvidin 3,5-di-*O*-glucoside) was suggested to be a good indicator for varietal origin and wine quality. This statement seems to be correct unless the loci for *5GT* and *AMAT* are decoupled by recombination or mutation in one of the genes abolishes the correlation between 5-*O*-glucosylation and methyl anthranilate formation. A recent success of grape breeders eliminating, for example, the "foxy" taste from their breeding material confirms such events and opens a new chapter for grapevine breeding (*30*). In view of the tremendous progress that has been achieved, malvin can no longer be considered as a clear-cut diagnostic tool for describing wine quality. With knowledge of the mutations in the *5GT* gene, decoupling of malvin from off-flavor formation will be shown within the next generation of grapevine cultivars.

In conclusion, we provide the biochemical foundation for the lack of anthocyanin 3,5-di-*O*-glucosides in *V. vinifera* grapes. The outcome of this study has a significant impact on the classification of *Vitis* varieties, for the determination of ancestry of hybrids, and the evaluation of products derived thereof. Knowledge of the crucial underlying mutational events supports the development of highly specific genetic markers for genotyping and marker-assisted selection in breeding. Therefore, this work contributes to the ongoing change in grapevine breeding moving from empirical crossings to sophisticated planning of a desired genotype.

ABBREVIATIONS USED

AMAT, anthraniloyl-CoA:methanol anthraniloyl transferase; LC-MS, liquid chromatography−mass spectrometry; SSR, simple sequence repeat; BAC, bacterial artificial chromosome.

ACKNOWLEDGMENT

We thank Farhah Assaad for correcting the manuscript.

Supporting Information Available: Oligonucleotide primers used for construct assembly (Table S1), product formation demonstrated by TLC analysis (Figure S1), product formation (cyanidin 3,5-di-*O*-glucoside) demonstrated by LC-MS analysis (Figure S2), product formation (cyanidin 3-*O*-rutinoside 5-*O*-glucoside) demonstrated by LC-MS analysis (Figure S3), product ion spectra of products (Figure S4), and conservation of the phenylalanine and the corresponding leucine residue in the amino acid sequences of glucosyltransferases (Figure S5).This material is available free of charge via the Internet at http://pubs.acs.org.

LITERATURE CITED

(1) Manen, J.-F.; Bouby, L.; Dalnoki, O.; Marinval, P.; Turgay, M.; Schlumbaum, A. Microsatellites from archaeological *Vitis vinifera* seeds allow a tentative assignment of the geographical origin of ancient cultivars. *J. Archaeol. Sci.* **2003**, *30*, 721–729.

(2) Zohary, D.; Spiegel-Roy, P. Beginnings of fruit growing in the Old World. *Science* **1975**, *187*, 319–327.

(3) Grassi, F.; Labra, M.; Imazio, S.; Spada, A.; Sgorbati, S.; Scienza, A.; Sala, F. Evidence of a secondary grapevine domestication centre detected by SSR analysis. *Theor. Appl. Genet.* **2003**, *107*, 1315–1320.

(4) Arroyo-García, R.; Ruiz-García, L.; Bolling, L.; Ocette, R.; López, M. A.; Arnold, C.; Ergul, A.; Söylemezoğlu, G.; Uzun, H. I.; Cabello, F.; Ibáñez, J.; Aradhya, M. K.; Atanassov, A.; Atanassov, I.; Balint, S.; Cenis, J. L.; Costantini, L.; Gorislavets, S.; Grando, M. S.; Klein, B. Y.; McGovern, P. E.; Merdinoglu, D.; Pejic, I.; Pelsy, F.; Primikirios, N.; Risovannaya, V.; Roubelakis-Angelakis, K. A.; Snoussi, H.; Sotiri, P.; Tamhankar, S.; This, P.; Troshin, L.; Malpica, J. M.; Lefort, F.; Martinez-Zapater, J. M. Multiple origins of cultivated grapevine (*Vitis vinifera* L. ssp. *sativa*) based on chloroplast DNA polymorphisms. *Mol. Ecol.* **2006**, *15*, 3707–3714.

(5) This, P.; Lacombe, T.; Thomas, M. R. Historical origins and genetic diversity of wine grapes. *Trends Genet.* **2006**, *22*, 511–519.

(6) Shiraishi, M.; Yamada, M.; Mitani, N.; Ueno, T. A rapid determination method for anthocyanin profiling in grape genetic resources. *J. Jpn. Soc. Hortic. Sci.* **2007**, *76*, 28–35.

(7) Mazzuca, P.; Ferranti, P.; Picariello, G.; Chianese, L.; Addeo, F. Mass spectrometry in the study of anthocyanins and their derivatives: differentiation of *Vitis vinifera* and hybrid grapes by liquid chromatography/electrospray ionization mass spectrometry and tandem mass spectrometry. *J. Mass Spectrom.* **2005**, *40*, 83–90.

(8) Berente, B.; Reichenbächer, M.; Danzer, K. Improvement of the HPLC analysis of anthocyanins in red wines by use of recently developed columns. *Fresenius' J. Anal. Chem.* **2001**, *371*, 68–72.

(9) Goldy, R. G.; Maness, E. P.; Stiles, H. D.; Clark, J. R.; Wilson, M. A. Pigment quantity and quality characteristics of some native *Vitis rotundifolia* Michx. *Am. J. Enol. Vitic.* **1989**, *40*, 253–258.

(10) Heier, A.; Blass, W.; Dross, A.; Wittkowski, R. Anthocyanin analysis by HPLC/ESI-MS. *Am. J. Enol. Vitic.* **2002**, *53*, 78–86.

(11) Vidal, S.; Hayasaka, Y.; Meudec, E.; Cheynier, V.; Skouroumounis, G. Fractionation of grape anthocyanin classes using multilayer coil countercurrent chromatography with step gradient elution. *J. Agric. Food Chem.* **2004**, *52*, 713–719.

(12) Urban, P.; Werck-Reichhart, D.; Teutsch, H. G.; Durst, F.; Regnier, S.; Kazmaier, M.; Pompon, D. Characterization of recombinant plant cinnamate 4-hydroxylase produced in yeast. Kinetic and spectral properties of the major plant P450 of the phenylpropanoid pathway. *Eur. J. Biochem.* **1994**, *222*, 843–850.

(13) Seitz, C.; Ameres, S.; Forkmann, G. Identification of the molecular basis for the functional difference between flavonoid 3′-hydroxylase and flavonoid 3′,5′-hydroxylase. *FEBS Lett.* **2007**, *581*, 3429–3434.

(14) Guex, N.; Peitsch, M. C. SWISS-MODEL and the Swiss-PdbViewer: an environment for comparative protein modeling. *Electrophoresis* **1997**, *18*, 2714–2723.

(15) Shao, H.; He, X.; Achine, L.; Blount, J. W.; Dixon, R. A.; Wang, X. Crystal structures of a multifunctional triterpene/flavonoid glycosyltransferase from *Medicago truncatula*. *Plant Cell* **2005**, *17*, 3141–3154.
(16) Ford, C. M.; Boss, P. K.; Høj, P. B. Cloning and characterization of *Vitis vinifera* UDP-glucose:flavonoid 3-*O*-glucosyltransferase, a homologue of the enzyme encoded by the maize *Bronze-1* locus that may primarily serve to glucosylate anthocyanidins *in vivo*. *J. Biol. Chem.* **1998**, *273*, 9224–9233.
(17) Offen, W.; Martinez-Fleites, C.; Yang, M.; Kiat-Lim, E.; Davis, B. G.; Tarling, C. A.; Ford, C. M.; Bowles, D. J.; Davies, G. Structure of a flavonoid glucosyltransferase reveals the basis for plant natural product modification. *EMBO J.* **2006**, *25*, 1396–1405.
(18) Yamazaki, M.; Yamagishi, E.; Gong, Z.; Fukuchi-Mizutani, M.; Fukui, Y.; Tanaka, Y.; Kusumi, T.; Yamaguchi, M.; Saito, K. Two flavonoid glucosyltransferases from *Petunia hybrida*: molecular cloning, biochemical properties and developmentally regulated expression. *Plant Mol. Biol* **2002**, *48*, 401–411.
(19) Yamazaki, M.; Gong, Z.; Fukuchi-Mizutani, M.; Fukui, Y.; Tanaka, Y.; Kusumi, T.; Saito, K. Molecular cloning and biochemical characterization of a novel anthocyanin 5-*O*-glucosyltransferase by a mRNA differential display for plant forms regarding anthocyanin. *J. Biol. Chem.* **1999**, *274*, 7405–7411.
(20) Nakatsuka, T.; Sato, K.; Takahashi, H.; Yamamura, S.; Nishihara, M. Cloning and characterization of the UDP-glucose:anthocyanin 5-*O*-glucosyltransferase gene from blue-flowered gentian. *J. Exp. Bot.* **2008**, *59*, 1241–1252.
(21) Imayama, T.; Yoshihara, N.; Fukuchi-Mizutani, M.; Tanaka, Y.; Ino, I.; Yabuya, T. Isolation and characterization of a cDNA clone of UDP-glucose:anthocyanin 5-*O*-glucosyltransferase in *Iris hollandica*. *Plant Sci.* **2004**, *167*, 1243–1248.
(22) Tohge, T.; Nishiyama, Y.; Hirai, M. Y.; Yano, M.; Nakajima, J.; Awazuhara, M.; Inoue, E.; Takahashi, H.; Goodenowe, D. B.; Kitayama, M.; Noji, M.; Yamazaki, M.; Saito, K. Functional genomics by integrated analysis of metabolome and transcriptome of *Arabidopsis* plants over-expressing an MYB transcription factor. *Plant J.* **2005**, *42*, 218–235.
(23) Lund, O.; Nielsen, M.; Lundegaard, C.; Worning, P. CPHmodels 2.0: X3M a Computer Program to Extract 3D Models. *Abstract, CASP5 Conference*; 2002, A102 (http://www.cbs.dtu.dk/services/CPHmodels/).
(24) Li, L.; Modolo, L. V.; Escamilla-Trevino, L. L.; Achnine, L.; Dixon, R. A.; Wang, X. Crystal structure of *Medicago truncatula* UGT85H2 - insights into the structural basis of a multifunctional (iso)flavonoid glycosyltransferase. *J. Mol. Biol.* **2007**, *370*, 951–963.
(25) He, X.-Z.; Wang, X.; Dixon, R. A. Mutational analysis of the *Medicago* glycosyltranferase UGT71G1 reveals residues that control regioselectivity for (iso)flavonoid glycosylation. *J. Biol. Chem.* **2006**, *281*, 34441–34447.
(26) Cartwright, A. M.; Lim, E.-K.; Kleanthous, C.; Bowles, D. J. A kinetic analysis of regiospecific glucosylation by two glycosyltransferases of *Arabidopsis thaliana*: domain swapping to introduce new activities. *J. Biol. Chem.* **2008**, *283*, 15724–15731.
(27) Wang, J.; De Luca, V. The biosynthesis and regulation of biosynthesis of Concord grape fruit esters, including 'foxy' methylanthranilate. *Plant J.* **2005**, *44*, 606–619.
(28) Moio, L.; Etievant, P. X. Ethyl anthranilate, ethyl cinnamate, 2,3-dihydrocinnamate, and methyl anthranilate: four important odorants identified in Pinot noir wines of Burgundy. *Am. J. Enol. Vitic.* **1995**, *46*, 392–398.
(29) Aubry, V.; Etiévant, P. X.; Giniès, C.; Henry, R. Quantitative determination of potent flavor compounds in Burgundy Pinot Noir wines using a stable isotope dilution assay. *J. Agric. Food Chem.* **1997**, *45*, 2120–2123.
(30) Robinson, J. Regent. In *Oxford Companion to Wine*, 3rd ed.; Oxford University Press: Oxford, U.K., 2006; pp 565.
(31) Thompson, J. D.; Gibson, T. J.; Plewniak, F.; Jeanmougin, F.; Higgins, D. G. The CLUSTAL_X windows interface: flexible strategies for multiple sequence alignment aided by quality analysis tools. *Nucleic Acids Res.* **1997**, *25*, 4876–4882.

Received for Review January 14, 2009. Revised manuscript received March 13, 2009. Accepted March 18, 2009.